

# Report on Project FA2386-09-1-4082

## “Slow Wave Enhanced Antennas at RF and Optical Frequencies”

### Research goals

To study novel structures of antennas enhanced with slow waves. To improve the performance and reduce the size of an antenna at RF frequencies by using metamaterial-based slow wave, and to develop highly-sensitive optical sensors by utilizing a combination of slow wave and optical nano-antennas.

### Summary of research results

1. A cavity with double nanobeams structure has been designed and the slow light mode has been identified at the cut-off wavelength of a band structure with nearly flat  $\omega(k)$  dispersion. The cavity has been fabricated successfully and its performance as a high resolution sensor has been characterized.

2. By introducing complementary split ring resonators (CSRR), complementary electric-LC resonators (CELC), or DGSs (defected ground structure), we have designed slow wave antennas to miniaturize the size of the antenna.

3. Micro-Ring-Resonator (MRR) with slow light effect has been designed and fabricated. The resonant wavelength shifts according to the concentration of the glucose solution flowing above the sensor region.

4. A nano-cavity antenna placed a certain distance away from the input surface of a nano-slit aperture milled in a metal film has been found to be able to greatly enhance the light transmission efficiency.

5. We have observed and studied some interesting phenomena associated with nearly zero index, which usually has an implication of slow group velocity (or very large phase velocity). For example, we have squeezed electromagnetic energy by using a dielectric split ring inside a permeability-near-zero metamaterial.

### Research results in details

#### 1. Slot slow light sensor

Miniaturization of label-free optical sensors is of particular interest for realizing ultracompact lab-on-a-chip applications with dense arrays of functionalized spots for multiplexed sensing, which may lead to portable, low cost and low power devices. So far, many kinds of photonic crystal (PhC) sensors based on regular PhCs, PhC waveguides and PhC cavities have been demonstrated. We studied some cavities realized in double nanobeams patterned with a one-dimensional lattice of holes. To measure the sensitivity of our structures, the samples were infiltrated with distilled water and sugar/water solution separately, with known refractive indices. High sensitivity is achieved on these structures in our experiment. The structures are promising for application after improving the Q factor.

## Report Documentation Page

Form Approved  
OMB No. 0704-0188

Public reporting burden for the collection of information is estimated to average 1 hour per response, including the time for reviewing instructions, searching existing data sources, gathering and maintaining the data needed, and completing and reviewing the collection of information. Send comments regarding this burden estimate or any other aspect of this collection of information, including suggestions for reducing this burden, to Washington Headquarters Services, Directorate for Information Operations and Reports, 1215 Jefferson Davis Highway, Suite 1204, Arlington VA 22202-4302. Respondents should be aware that notwithstanding any other provision of law, no person shall be subject to a penalty for failing to comply with a collection of information if it does not display a currently valid OMB control number.

1. REPORT DATE

**21 JUL 2010**

2. REPORT TYPE

**Final**

3. DATES COVERED

**07-05-2009 to 06-05-2010**

4. TITLE AND SUBTITLE

**Slow Wave Enhanced Antennas at RF and Optical Frequencies**

5a. CONTRACT NUMBER

**FA23860914082**

5b. GRANT NUMBER

5c. PROGRAM ELEMENT NUMBER

6. AUTHOR(S)

**Sailing He**

5d. PROJECT NUMBER

5e. TASK NUMBER

5f. WORK UNIT NUMBER

7. PERFORMING ORGANIZATION NAME(S) AND ADDRESS(ES)

**Royal Institute of Technology, Teknikringen 33, Stockholm, Sweden, SW, 100 44**

8. PERFORMING ORGANIZATION REPORT NUMBER

**N/A**

9. SPONSORING/MONITORING AGENCY NAME(S) AND ADDRESS(ES)

**Asian Office of Aerospace Research & Development, (AOARD), Unit 45002, APO, AP, 96338-5002**

10. SPONSOR/MONITOR'S ACRONYM(S)

**AOARD**

11. SPONSOR/MONITOR'S REPORT NUMBER(S)

**AOARD-094082**

12. DISTRIBUTION/AVAILABILITY STATEMENT

**Approved for public release; distribution unlimited**

13. SUPPLEMENTARY NOTES

14. ABSTRACT

**During the course of this grant, novel structures of antennas enhanced with slow waves was studied. The goal of this research is to improve the performance and reduce the size of an antenna at RF frequencies by using metamaterial-based slow wave, and to develop highly-sensitive optical sensors by utilizing a combination of slow wave and optical nano-antennas. The following results were obtained: 1. A cavity with double nanobeams structure has been designed and the slow light mode has been identified at the cut-off wavelength of a band structure with nearly flat  $\omega(k)$  dispersion. The cavity has been fabricated successfully and its performance as a high resolution sensor has been characterized. 2. By introducing complementary split ring resonators (CSRR), complementary electric-LC resonators (CELC), or DGSs (defected ground structure), we have designed slow wave antennas to miniaturize the size of the antenna. 3. Micro-Ring-Resonator (MRR) with slow light effect has been designed and fabricated. The resonant wavelength shifts according to the concentration of the glucose solution flowing above the sensor region. 4. A nano-cavity antenna placed a certain distance away from the input surface of a nano-slit aperture milled in a metal film has been found to be able to greatly enhance the light transmission efficiency. 5. We have observed and studied some interesting phenomena associated with nearly zero index, which usually has an implication of slow group velocity (or very large phase velocity). For example, we have squeezed electromagnetic energy by using a dielectric split ring inside a permeability-near-zero metamaterial.**

15. SUBJECT TERMS

**Metamaterials, Antennas, Electromagnetics**

16. SECURITY CLASSIFICATION OF:			17. LIMITATION OF ABSTRACT <b>Same as Report (SAR)</b>	18. NUMBER OF PAGES <b>7</b>	19a. NAME OF RESPONSIBLE PERSON
a. REPORT <b>unclassified</b>	b. ABSTRACT <b>unclassified</b>	c. THIS PAGE <b>unclassified</b>			

**Standard Form 298 (Rev. 8-98)**  
Prescribed by ANSI Std Z39-18

Fig. 1.1(a) shows the Scanning Electron Microscope (SEM) image of the waveguide. Fig. 1.1(b) shows the PL spectrum of the structure with the infiltration of distilled water. The peak at 1386.5 nm is the slot mode, which corresponds to an even mode at the cut-off wavelength of a band structure with nearly flat  $\omega(k)$  dispersion, i.e., in the slow light regime. Fig. 1.1(c) shows the PL spectrum of the same waveguide with the infiltration of sugar/water solution. The peak redshifts to 1392.4 nm. This gives a sensitivity of  $7 \cdot 10^2$  nm /RIU.

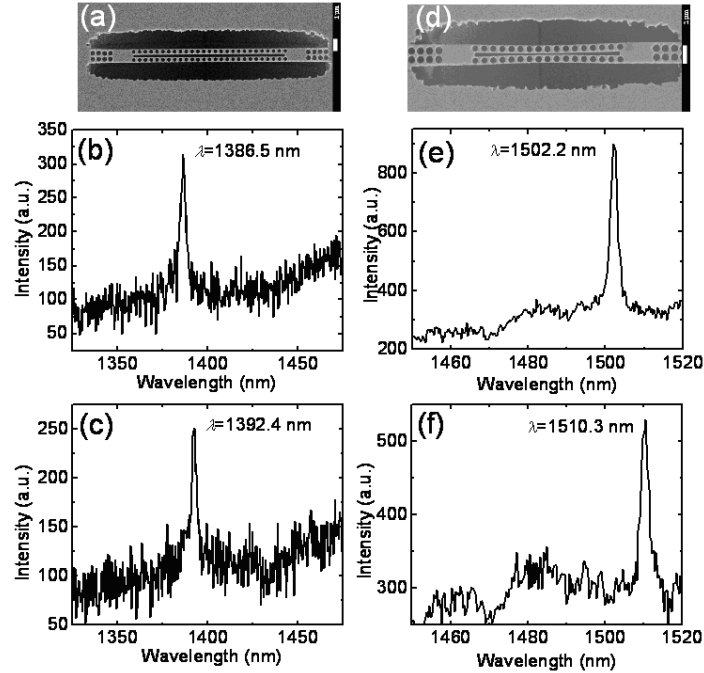


Fig. 1.1 SEM image of (a) an InGaAsP PhC nanobeam slow light slot waveguide, (b) a cavity type InGaAsP PhC nanobeam slow light slot waveguide; PL spectrum of the waveguide with the infiltration of (b), (e) distilled water, (c), (f) sugar/water solution.

Accidentally, we have a waveguide with stuck nanobeams, which is shown in Fig. 1.1(d). The nanobeams bend inward which makes the slot region narrow in the central part and a cavity is formed. Fig. 1.1(e) shows the PL spectrum of the cavity with the infiltration of distilled water. The peak at 1502.2 nm is the slot cavity mode. Fig. 1.1(f) shows the PL spectrum of the same structure with the infiltration of sugar/water solution. The peak redshifts to 1510.3 nm. This gives a high sensitivity of about 900 nm/RIU.

## 2. Slow wave RF antenna

(a) By introducing complementary split ring resonators (CSRR) and complementary electric-LC resonators (CELC), we can design a slow wave antenna to miniaturize the size of the antenna. The effective medium approach is applied here to extract the effective permittivity of CSRR and the effective permeability of CELC. As shown in Fig. 2.1, the resonant frequency of the CSRR is 1.7GHz and that of CELC is 2.6GHz.

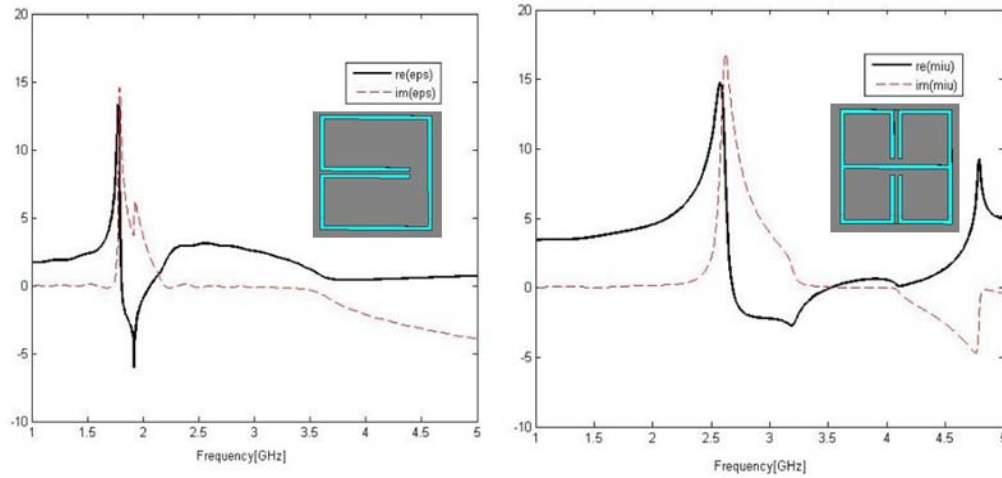


Figure 2.1. (a) Effective permittivity of CSRR with resonance frequency of 1.7GHz (b) Effective permeability of CELC with resonance frequency of 2.6GHz

From the measured  $S_{11}$  of the antenna in Fig. 2.2, three working bands—1.956GHz, 2.96GHz and 4.05GHz have been observed. The first band is due to the resonant of CSRR and the second is due to the resonant of CELC. The large slope and negative band of  $\epsilon$  and  $\mu$  curve of CSRR and CELC brings slow wave factor to the antenna, which makes the antenna working at much lower frequency as compared with a conventional antenna of same size.

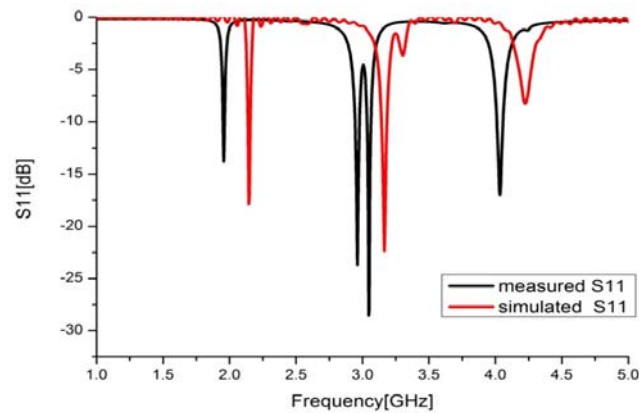


Figure 2.2. Reflection coefficient of the slow wave antenna

Besides, there is a double-close-peak near the 2.96GHz band, which results from the coupling between CSRR and CELC. Note here that only one element of the complementary metamaterial is etched on the ground plane, which aims to minimize the backward radiation.

(b) A new design of isotropic DGS, based on dumbbell shape is proposed with good miniaturizing effect. As shown in Figure 2.3, the proposed DGS has the largest slope in the slow wave region as compared with cross and dumbbell ones.

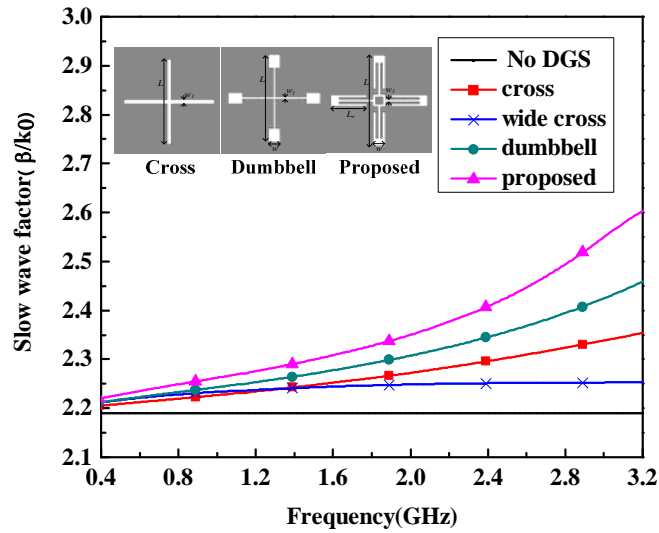


Figure 2.3. Slow wave factor as a function of frequency for different DGSs.

The proposed DGS structure is used to design polarization switchable antenna operating at two linear polarizations along the x- and y-direction, respectively. The antenna structure with biasing circuit is shown in Figure 2.4. The planar artificial cells have quasi-lumped structures, with no use for extra surface mounted devices or via holes. The PIN diode is soldered between the terminal of the feed line and the 2.5mm×2.5mm pad with a ground via. A 5pF capacitor is inserted at a position of 10mm away from the feed point to isolate DC current. A  $\lambda/4$  length stub of 18.78mm is used as AC block.

When the diode is switched on, the feed line is inductively coupled with the radiation patch, so an electric current along x-axis is produced. Instead, when the diode is switched off, the feed line is capacitively coupled with the radiation patch, and the current flows along the y-axis.

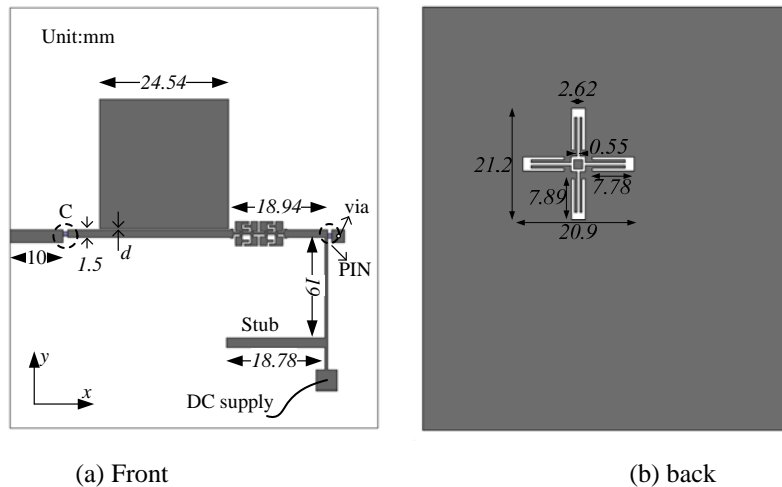


Figure 2.4 . Geometry of the proposed switchable antenna.

As shown in Figure 2.5, the simulated resonant frequencies in the ON and OFF states are equal to 2.23 and 2.25 GHz, respectively. The slight frequency difference is made to keep good cross polarization in each state, and the measured reflection coefficients agree well with the

simulated ones.

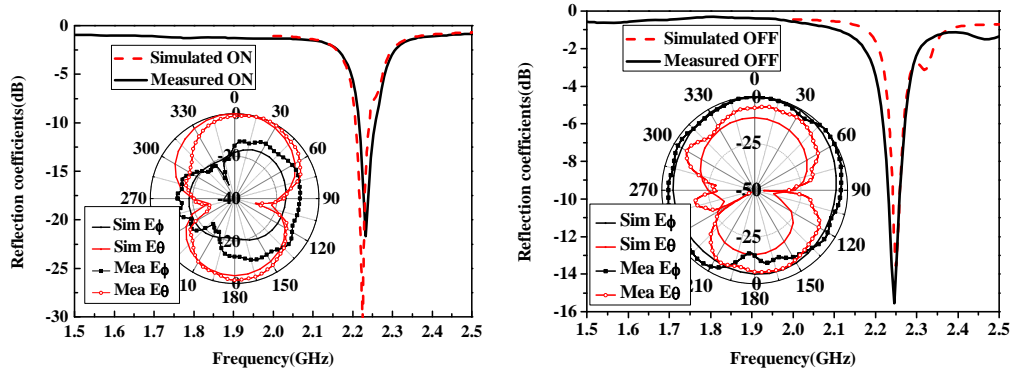


Figure 2.5. Measured and simulated reflection coefficients in ON and OFF states.

The  $xz$  plane radiation pattern is shown as the insets of Figure 2.5. When the diode is switched on,  $E_\phi$  is the main polarization component, while the cross polarization  $E_\theta$  -component is below -18 and -15dB in simulation and measurement, respectively. When the PIN diode is tuned to OFF state, the cross polarization level is -10 and -6dB in simulation and measurement, respectively. The cross polarization in the OFF state is worse than that of the ON state, which is caused by the weak capacitive coupling between the feed line and the patch.

### 3. MRR slow light sensor

When the refractive index for the upper cladding of the Micro-Ring-Resonator (MRR) is changed, the resonant wavelength will shift accordingly. By using the glucose solution as the upper cladding, refractive index change of the glucose solution can be detected. The glucose solution is pumped through the pipe to the micro-fluid channel above the MRR sensor and flow out through the pipe. We use micro-fluid channel to guide the glucose solution. As the concentration and the refractive index are linear to each other at the low concentration limit, one can detect the relative concentration variation by monitoring the resonant wavelength change.

In our MRR sensing system, waves propagate from one resonator to another through energy coupling, the effective velocity is much lower (slow wave), bringing to a higher sensitivity. The experimental set-up and sensing result are shown in Fig. 3.1.

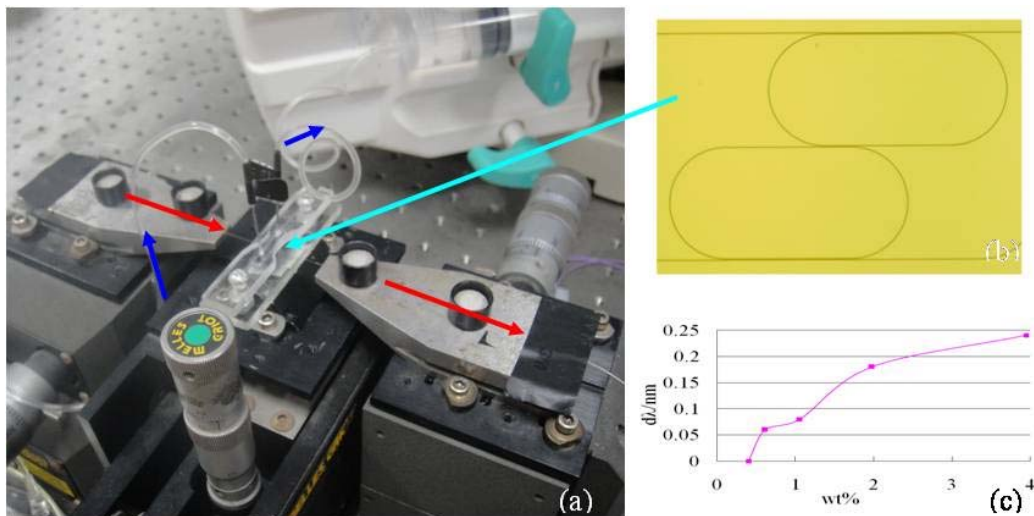


Figure 3.1 (a) The measurement setup for the MRR sensing system. The red arrows show the light path while the blue arrows shows the liquid path; (b) the microscopy picture of the double MRR sensor; (c) The wavelength shift for the MRR as the concentration of the glucose solution varies.

#### 4. Optical nano-cavity antenna

We have given a clear physical explanation for the dependence of the transmission on the slit-to-groove distance. We have shown that the influence to the transmission comes from three parts: the groove-generated SPW, the incident wave and the nano-slit-generated SPW. The groove-generated SPW is the main factor determining the local field distribution around the nano-slit opening.

Intuitively, a metallic nano-strip over the nano-slit seems to block the incident light. However, through the formation of a resonant nano-cavity antenna, the metallic nano-strip can assist to couple more incident light into the nano-slit and thus enhance the transmission. The field distribution is shown in Fig. 4.1.

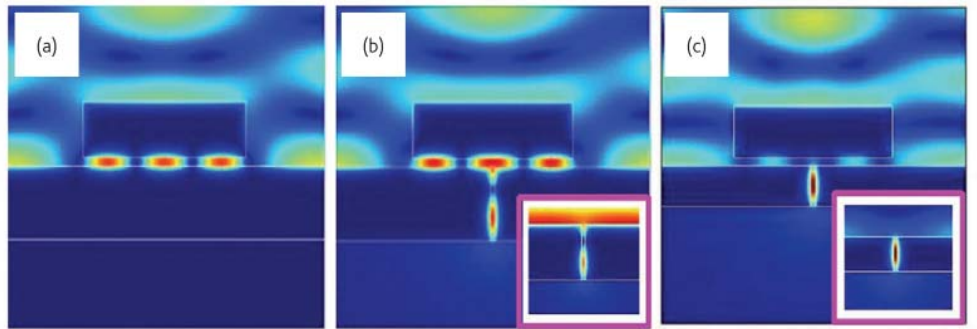


Figure 4.1. Distributions of  $|H_y|$  for a horizontal resonant MIM cavity ( $W_p = 1 \mu\text{m}$ ) (a), and a horizontal resonant cavity over a non-resonant nano-slit (b) or a resonant nano-slit (c). The insets in (b) and (c) show the  $|H_y|$  distributions for the corresponding cases of a bare nano-slit.

The light transmission enhanced by a single nano-antenna is still not high enough. This can be improved by replacing the single nano-antenna with an array of nano-antennas, as shown in Fig. 4.2.

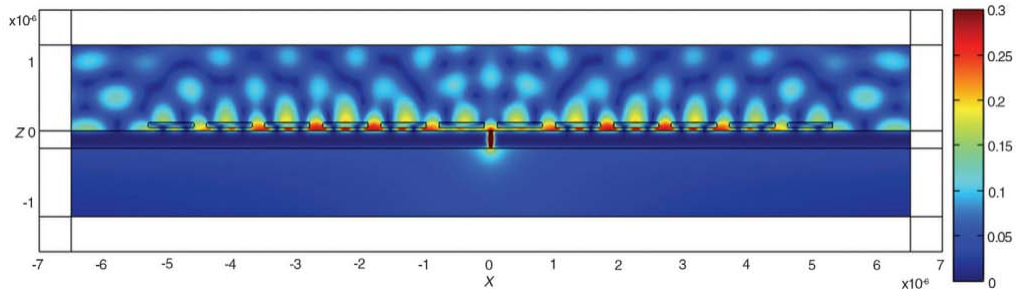


Figure 4.2. Distributions of  $|H_y|$  for the metallic nano-slit assisted by an array of nano-cavity antennas.

5. A metamaterial with nearly zero index is usually associated to slow group velocity (or very large

phase velocity). We have proposed an electromagnetic energy squeezing mechanism based on the special properties of permeability-near-zero metamaterials. We found that nearly no energy stream can enter a simply connected conventional dielectric material positioned inside a permeability-near-zero material. When the dielectric domain is shaped as a split ring (with a gap opened) surrounding a source, the electromagnetic energy generated by the source is forced to propagate through the gap. When the gap is narrow, the energy stream density becomes very large and makes the magnetic field enhanced drastically in the gap (see Fig. 5.1). The narrow gap can be long and bended. This provides us a method to obtain strong magnetic field without using resonance enhancement.

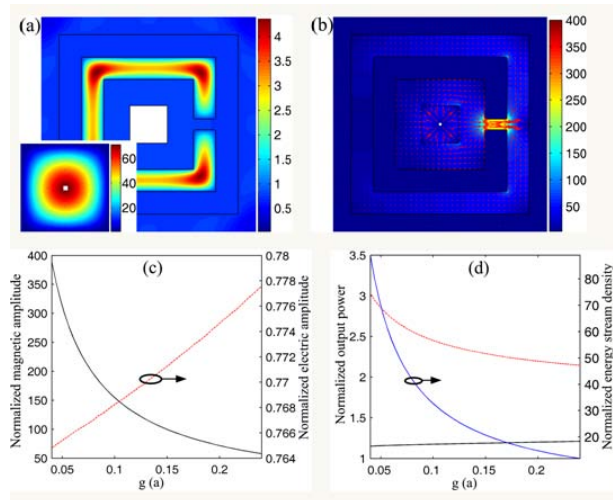


Figure 5.1. Energy squeezing in a permeability-near-zero metamaterial

**List of published papers that the AOARD grant is acknowledged:**

[1] Y. Cui and S. He, *Opt. Express*, 17 (16) 13995-14000, 2009.  
 [2] S. He, et al, *Materials Today*, 12 (12), 16-24, 2009.  
 [3] Y. Cui, J. Hu, S. He, *JOURNAL OF THE OPTICAL SOCIETY OF AMERICA B-OPTICAL PHYSICS*, 26(11), 2131-2135, NOV 2009.  
 [4] Y. Jin, P. Zhang, and S. He, *PHYSICAL REVIEW B*, 81(8), 085117, FEB 2010.

A few other papers are in press or under review.